Indian. J Met. Hydrol. Geophys. (1975), 26, 3, 334-344

551.501.7 : 551.55

Generation of very high supergeostrophic winds using a new form of oscillating eddy viscosity profile in a barotropic planetary boundary layer*

V. V. SHIRVAIKAR

Bhabha Atomic Research Centre, Bombay

ABSTRACT. Observed diurnal variation of wind in the planetary boundary layer is characterised by two features, *viz.*, the 'elliptical' pattern described by the horizontal wind vector and occurrence of supergeostrophic winds. In summer, these may exceed $1 \cdot 7G$ where G is the geostrophic wind. Theoretical work has produced qualitatively the elliptical patterns of wind vector, but the supergeostrophic winds have been limited to $1 \cdot 35\,G$. In this paper, an expression based on the eddy conductivity data from Cedar Hill Texas in a 434 m layer is analysed to obtain a new expression for the eddy viscosity $K(z, t)$. Departure from convention is made in that, Fourier analysis is made on log K instead of on K, giving an expression of type, $K(z,t) = K_0(z) \exp [a(z) \cos \omega [t - \epsilon (z)]]$ to give all positive values of K. Numerical solution of equation of motion (for horizontal wind) in a barotropic planetary boundary layer are obtained using the above form of $K(z,t)$. Next, analytic solution of the momentum equation is obtained for the simplest form of the above expression for $K(z, t)$, *viz.*, $K = K_0 \exp(a \cos \omega t)$ where K_0 and a are constants. It is shown that if we use high values of a as shown by observed oscillations of K at Manor Texas, supergeostropic winds as high as $1 \cdot 75\,G$ can be obtained. Finally, using the same analytic solution method, dependence of the wind oscillations on various parameters is discussed.

1. Introductory review

Diurnal variations of wind observed in the planetary boundary layer show the wind vector describing an approximately elliptical pattern (Wagner 1939; Blackadar 1957; Buajitti and Blackadar 1957). The size of the 'ellipse' is largest at a few hundred metres. The orientation of the semi-major axis of ellipses observed by Buajitti and Blackadar (*loc. cit.*) at Oklahoma City was mainly in the direction of the mean wind. However, the hodographs of wind given by Wagner (*loc. cit.*) for Houston, Texas do not show this feature.

Another observed feature of the diurnal wind variation is the occurrence of predawn wind maxima in the vertical profiles, of magnitude exceeding the geostrophic value G. At the Great Plains in USA where the density of observational data is large, the predawn supergeostrophic wind maxima, often called low level jets, attain values as high as $1.7\,G$. Some of the examples cited by Blackadar (1957) show wind maxima of about $1.56\,G$ in autumn at 39° latitude (Maryland, USA) and $1.3\,G$ in winter at 30° in Texas, USA. A most striking example is that of the mean jet at Fort Lamy in Africa equal to about three times the geostrophic wind in winter.

The equation of motion in a barotropic planetary boundary layer is—

$$\frac{\partial u}{\partial t} = fv + \frac{\partial}{\partial z}\left\{ K(z,t) \frac{\partial u}{\partial z} \right\}$$

$$\frac{\partial v}{\partial t} = f(G - u) + \frac{\partial}{\partial z}\left\{ K(z,t) \frac{\partial v}{\partial z} \right\} \quad (1)$$

where the x-axis is oriented in the geostrophic wind direction and the terms have their usual meaning. When G is constant, it is seen that the solutions and hence the supergeostrophic wind will depend only on the form of the eddy viscosity $K(z, t)$.

Several forms of $K(z, t)$ have been used by earlier workers to study the nature of diurnal variations. The forms were generally separable in height and time, *viz.*, $K(z, t) = g(z)\ h(t)$. Buajitti and Blackadar (1957) and Paegle (1970) used the simplest form of $h(t) = 1 + \alpha \cos \omega t$ with $g(z) =$ const., when analytic solutions were sought. Here α is the amplitude < 1 and ω refers to 24-hr period. Haltiner (1959) used one more harmonic but had to resort to numerical techniques. He modelled $g(z)$ after the Leipzig profile (Lettau 1950) and also gave another expression for K based on the work of McBride (1960) and Haltiner (1960, 1961).

Mention must also be made of Estoque's (1963) non-analytical specification of $K(z, t)$ where K, is given by surface layer relations upto a height of 50 m which he takes to be the height of the constant stress surface layer. From here onwards upto an assumed boundary layer of 2050 m K falls linearly to zero.

*Based on the Ph. D. Thesis by the author, Bombay Univ. 1971.

All the solutions showed qualitative agreement with observed variations in that they are elliptical but have failed to give supergeostrophic wind maxima greater than 1.35 G, *i.e.*, less than the observed.

Holton (1964) has taken into account diurnal variation due to thermal winds caused by a sloping terrain. Though the amplitudes of wind oscillation given by Holton for 30° latitude are comparable to the observed variations at 37°, drastic reduction in the amplitude has been found by Paegle (*loc. cit.*) when calculation was made for 37° itself.

One of the main difficulties in obtaining an adequate form of $K\ (z,\ t)$ is that any theoretical formulation becomes well nigh impossible in absence of constraints, *e.g.*, that of constancy of shear stress, with height as is used in the first few tens of metres of the surface layer. Thus the use of observational data for formulating forms of $K\ (z,\ t)$ becomes imperative.

Though data on diurnal variation of eddy viscosity are scarce, published data are available on eddy conductivity which often may be used interchangeably with eddy viscosity, within a layer of 434 m which forms a significant part of the planetary boundary layer. These are from the 434 m Cedar Hill Tower at Texas in spring and winter and have been published by Wong and Brundidge (1966). It is possible to use these data to obtain an empirical analytic expression for $K\ (z,\ t)$ valid within 434 m and also beyond, albeit by extrapolation based on indirect evidence of the behaviour of certain mean properties of $K\ (z,\ t)$.

The purpose of this paper is to obtain an empirical expression for $K\ (z,\ t)$ as outlined earlier and use it to investigate whether it is capable of generating the observed magnitudes of the supergeostrophic winds. Later, a method of obtaining the solution of Eq. (1) for $K\ (z,\ t) = K_0\, h(t)$ where $h(t)$ is *any* oscillating function will also be given.

2. Fourier representation of Cedar Hill data

The Cedar Hill data is in the form of half hourly points which are averages of six determinations in winter and five in summer respectively, at four heights : 9, 134, 284 and 434 m (levels designated Nos. 1, 6, 12 and 18). Some points are missing and the negative value of K observed during the analysis have been omitted. The diurnal variation of K is over about one order of magnitude.

The procedure followed here to obtain expressions for $K\ (z,\ t)$ was to fit empirical relations to the Fourier coefficients and phases obtained from the Fourier analysis of the Cedar Hill data, subject to certain boundary criteria. For the sake of simplicity and reducing computational efforts, it is desirable to truncate the series to first harmonic. One of the drawbacks in such truncation when the dependent variable has large amplitude (as for K) is that the truncated series often gives negative values of K in the region of $K_{\min.}$ To avoid this, the Fourier analysis was done on log K instead of K.

With the Fourier analysis on log K, we may write

$$K\ (z,\ t) = K_0\ (z)\ \exp\ [R_1\ (z) \cos\ \omega\ [t - \epsilon_1\ (z) + R_2(z) \cos\ 2\omega\ [t - \epsilon_2\ (z)] + \ldots.] \quad (2)$$

where R_i and ϵ_i are the amplitudes and phases respectively of

$$\log\ \{K\ (z,\ t)\}\ \text{and}\ K_0\ (z) = \exp\{R_0\ (z)\}$$

The first harmonic truncation will give

$$K\ (z, t) = K_0\ (z)\ \exp\ \{a\ (z)\ \cos\ \omega[t - \epsilon_1\ (z)]\} \quad (3)$$

Table 1 gives the amplitudes R_0 obtained from Fourier analysis on log K performed after smoothing the data. The table also shows the corresponding phases in hours (CST). For comparison, the corresponding parameters for Fourier analysis on K are also shown in the corresponding tables.

As far as the convergences of series is concerned, there was found no preference between the linear and exponential representation. However, the advantages regarding the first harmonic truncation are clear when we refer to the values of R_0 and R_1 at level 6 (134m) in the linear representation for Cedar Hill. Since $R_0 < R_1$, such a truncation will give negative values of K during part of the cycle, whereas the exponential form can never give negative K.

It must be noted that the amplitudes for the two representations are not the same. As can be seen from the following equivalence :

$$e^{a \cos \omega t} = I_0\ (a) + 2\ I_1\ (a) \cos\ \omega t + 2\ I_2\ (a) \cos\ 2\ \omega t + \ \ldots\ . \quad (4)$$

where I_n are modified Bessel functions of the first kind. Thus we see that the exponential representation automatically includes part of the higher harmonics. For $a \approx 1$, 3-4 harmonics are significant.

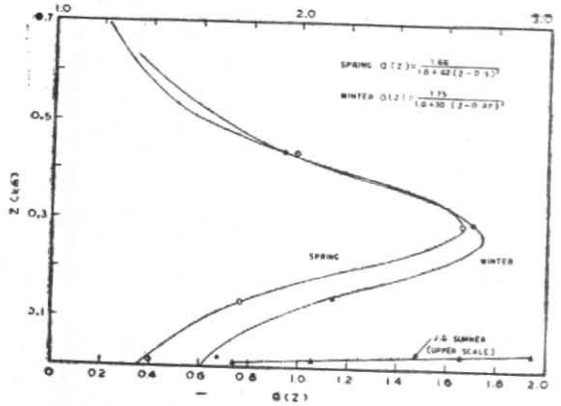

Fig.1. Variation of a (z) with height for spring and winter at Cedar Hill, Texas. The solid curves show the fitted expressions. Also are shown by solid triangles, the variation of $a(z)$ with height in summer at Manor Texas, from the data of Jehn & Gerhardt. These are much higher than for spring and winter, and upper scale should be used

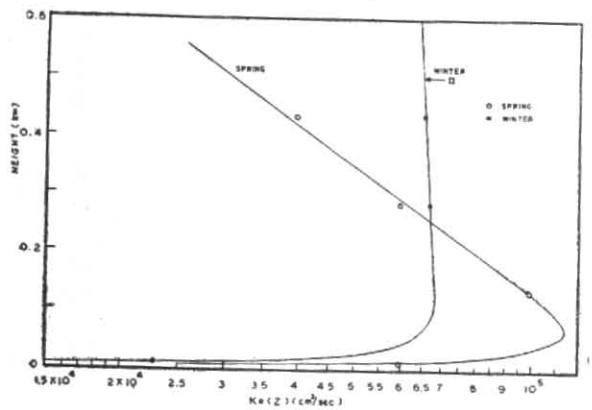

Fig. 2. Variation of $K_0(z)$ with height in spring and winter at Cedar Hill. The solid curves show the fitted expression

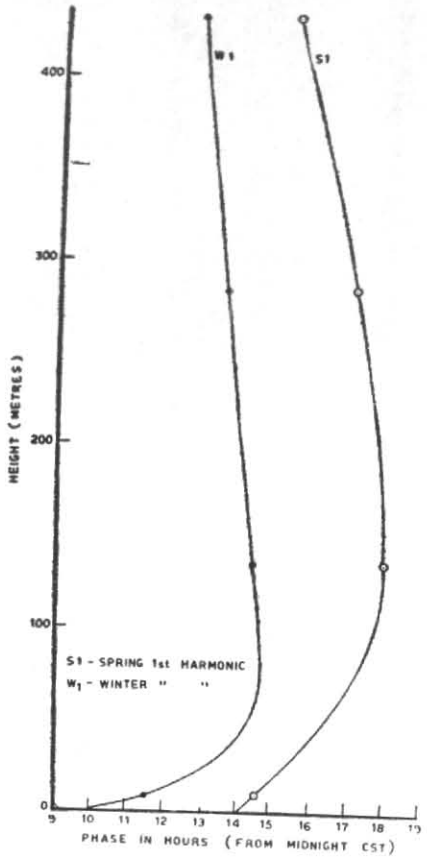

Fig. 3. Variation of phase of first harmonic with height in spring and winter at Cedar Hill. The curves show the fitted expressions

TABLE 1

Fourier components for log K and K from Cedar Hill

Level	Log K			K(cm²/sec)		
	R_0	R_1	ϵ_1 (hr CST)	R_0	R_1	ϵ_1 (hr CST)
			SPRING			
1	10·98	0·394	14·50	$4·91\times10^5$	$8·03\times10^5$	17·32
6	11·50	0·754	17·05	$1·69\times10^5$	$1·12\times10^5$	15·12
12	10·99	1·66	16·59	$1·48\times10^5$	$1·65\times10^5$	15·88
18	10·58	0·99	16·04	$9·33\times10^4$	$7·82\times10^4$	12·82
			WINTER			
1	10·03	0·669	11·49	$3·40\times10^4$	$2·01\times10^4$	12·66
6	10·80	1·142	14·26	$1·48\times10^5$	$1·85\times10^5$	15·03
12	11·11	1·696	13·55	$1·81\times10^5$	$1·93\times10^5$	13·70
18	11·07	0·949	12·72	$1·03\times10^5$	$7·23\times10^4$	12·01

3. Expression for $K(z, t)$ at Cedar Hill

In Figs. 1, 2 and 3 are plotted the values of $a(z)$, $K_0(z)$ and $\epsilon_1(z)$ respectively for the exponential representation. All these parameters first increase with height and then decrease monotonically.

Consider first the amplitude function $a(z)$ in Fig. 1. Several functions were tried for $a(z)$. Of these the Lorentz type function

$$a(z) = \frac{P}{1 + Q(z - z_m)^2} \tag{5}$$

where P, Q and z_m are constants, gave the best fit, with following values.

Spring :

$$P = 1.66,\ Q = 42\ \text{km}^{-2},\ z_m = 0.3\ \text{km}$$

Winter :

$$P = 1.75,\ Q = 30\ \text{km}^{-2},\ z_m = 0.27\ \text{km}$$

The functions are shown by solid curves in Fig. 2. Next, let us consider the function $K_0(z)$.

From Eq. (3) and (4) we note that the mean daily profile of eddy viscosity is given by

$$K(z). = K_0(z).\ I_0\{a(z)\} \tag{6}$$

Now, within the surface boundary layer of few tens of metres, the quantity $a(z)$ as seen from Fig. 2 does not change appreciably. For example in winter, $a(z)$ changes from 0.6 to 0.8 within the first 100 m. The corresponding values of I_0 are 1.092 and 1.166 respectively. Therefore, the term $I_0\{a(z)\}$ may be considered to be a constant ≈ 1. The expression for $K_0(z)$ therefore should satisfy the usually accepted lower boundary condition such that

(*i*) $K_0(z) = 0$ at the surface

(*ii*) $K_0(z)$ increases linearly near the surface.

Similarly, at the upper boundary since $a(z) \to 0$ and $I_0(a) \to 1$, and

(*iii*) $K_0(z)$ should tend to zero with increasing height after passing through a maximum (*cf.* Leipzig profile).

A suitable function for $K_0(z)$ satisfying all the three conditions, is

$$K_0(z) = K_0 \cdot (e^{-p_1 z} - e^{-p_2 z}) \tag{7}$$

In Fig. 2, Eq. (7) is fitted to the points in spring with the following values of the parameters.

Spring :

$K_0 = 1.54 \times 10^5\ \text{cm}^2/\text{sec}$,

$P_1 = 3.2\ \text{km}^{-1}$, $P_2 = 40\ \text{km}^{-1}$

With these parameters, $K_0(z)$ increases upto 60 m and then decreases.

Winter I :

In winter, the least square fit of Eq. (7) gave

$K_0 = 6.1 \times 10^4\ \text{cm}^2/\text{sec}$,

$P_1 = 0$, $P_2 = 51.8\ \text{km}^{-1}$

This implies that $K(z)$ remains constant beyond a few tens of metres above ground. However, the general behaviour of $K(z)$ in spring and that of Leipzig profile (in summer) suggest that a decrease of $K(z)$ with height may not be unrealistic. If, therefore, we assume a slow decrease of $K(z)$ with height as given by the two uppermost points for winter following parameters may be obtained.

Winter (II)

$K_0 = 7 \times 10^4\ \text{cm}^2/\text{sec}$,

$P_1 = 0.25\ \text{km}^{-1}$, $P_2 = 45\ \text{km}^{-1}$

These are not significantly different from Winter (I) parameters and shall be adopted here.

Lastly, we shall consider the phase term $\epsilon_1(z)$. The phase also first increases with height and then decreases linearly. This can be expressed as

$$\epsilon_1(z) = \epsilon_0 - z/\beta_1 - B_0\, e^{-z/\beta_2} \tag{8}$$

where ϵ_0, β_1, β_2 and B_0 are constants.

From Fig. 3 following values of the constants are determined.

Spring :

$\epsilon_0 = 21$ hr (CST), $\beta_1 = 0.085$ km/hr,

$B_0 = 7$ hr, $\beta_2 = 0.086$ km.

Winter :

$\epsilon_0 = 15.2$ hr (CST), $\beta_1 = 0{\cdot}18$ km/hr,

$B_0 = 5$ hr, $\beta_2 = 0.0215$ km.

It must be noted that the accuracy of B_0 and β_2 is comparatively poor due to lack of points. In some applications, the lowermost levels are not important and the exponential terms may be omitted.

The final expression for $K(z, t)$ is obtained by substituting expressions (5), (7) and (8) in Eq. (3).

Perhaps the greatest drawback of this expression is that it is based only on a set of four points and the formulation is entirely empirical

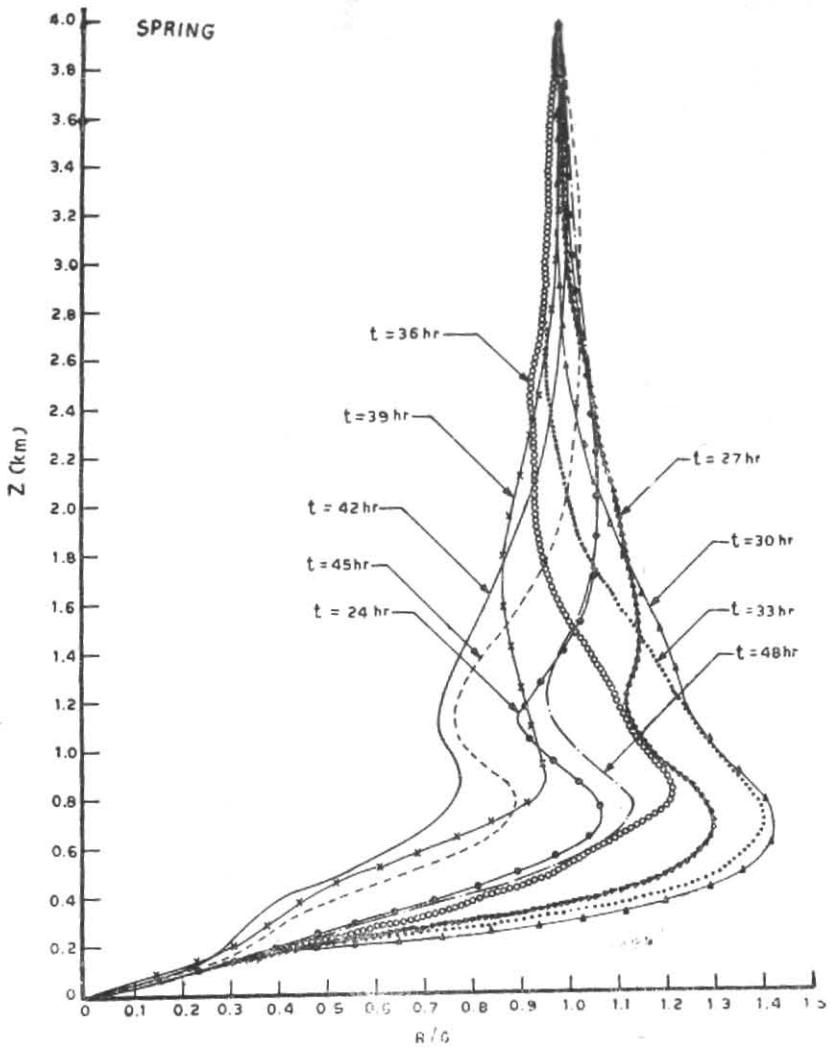

Fig. 4. Development of wind profiles for Cedar Hill $K(z, t)$ on second day of integration. The times indicated are CST

and therefore without a sound physical basis. However, the nature of variations with height are at least qualitatively in conformity with the Leipzig and Estoque profiles (*cf.* Fig. 8 later).

In the following, this profile will be used to calculate the variation of wind profiles with time and the magnitude of the maximum supergeostrophic excess.

4. Supergeostrophic winds, with Cedar Hill $K(z, t)$

Fig. 4 shows the calculated scalar wind profiles in spring obtained by using Cedar Hill $K(z, t)$ in Eq. (1). These were obtained from the *numerical* solutions of the Eq. (1) using the fourth order Runge Kutta method given by Gill (1952). The finite difference scheme used was the same as the linear scheme given by Haltiner (1959) but with $\triangle z = 0.05$ km and $\triangle t = 0.01$ hr with the following boundary conditions.

$$u_0 = v_0 = 0, \quad U_{81} = G = 1, \quad v_{81} = 0$$

where the zero suffix refers to the ground level and the geostrophic wind condition is clamped at 81st level (4 km). The latitude was 30°. The initial conditions were set as the Ekman distribution with eddy viscosity $= K_0$. The computations were done on a CDC 3600 computer.

The maximum supergeostrophic wind obtained is $1.42\ G$ at 0.6 km which is higher than the values obtained earlier. In winter this, calculated in a similar fashion, was $1.3\ G$ at 0300 CST and occurred at 0.5 km. The winter magnitude agrees with the average (16 profiles in January) jet of $1.3\ G$ at 0300 CST reported by Blackadar (1957) at San Antonio, Texas (29°45′) though the jet level was higher (0.9 km.)

High winds observed frequently in summer often exceeding $1.7\,G$ at Great Plains are not generated by the Cedar Hill $K\,(z,\,t)$. In this connection it is relevant to mention a criterion stated by Paegle (*loc. cit.*) : "*the theories of wind variation should predict the night-time predawn occurrence of speed maxima over the Great Plains. They should also be able to account for the 70% supergeostrophic excess which are sometimes observed*".

Cedar Hill $K(z,\,t)$ while generating the predawn jet does not account for the supergeostrophic excess of magnitude observed, though the values are higher than those deduced by earlier workers.

5. Low level jets in summer

The diurnal variation and the supergeostrophic excess are larger in summer for which Cedar Hill data were not available. However, if we refer to the data on K_H published by Jehn and Gerhardt (1950) for one day in summer at Manor Texas, for four levels between 5 and 35 m, some idea may be obtained as regards the magnitude of diurnal variation of K. The data were analysed in the same way as for Cedar Hill. The values of $a\,(z)$ thus obtained are plotted in Fig. 2. The remarkable feature of these is the magnitude. Whereas the maximum $a(z)$ for Cedar Hill in spring and winter were 1.6 and 1.8 respectively with an average of about 1.1 (diurnal variation by a factor of 9), the mean $a\,(z)$ for 35 m level itself is 2.35. When the corresponding levels are considered, the exponential amplitude $a\,(z)$ is about three times larger than the corresponding amplitudes in spring and winter. Despite this solitary observational reference, it seems to be safe to conclude that the diurnal oscillation of K is generally much higher in summer than in other seasons.

In absence of a complete specification of $K\,(z,\,t)$ in summer, we shall use the simple form of Eq. (3), *viz.*,

$$K = K_0\, e^{a\,\cos\,\omega t} \tag{9}$$

where K_0 and a are constants. Based on Paegle's study as well as the independent investigations by the author it may be stipulated that the results obtained by using Eq. (9) will not be significantly different whether K_0 is height dependent or not. In the following we shall make a study of diurnal variation of wind for different values of exponential amplitudes a. We shall give below a method of obtaining exact analytical solutions, albeit in integral form, of Eq. (1). In fact, the method is useful for any form of K that can be expressed as

$$K = K_0\, h(t) \tag{10}$$

where $h\,(t)$ is any oscillatory function. The method will, therefore, also be used to obtain solutions of (1) with a linear cosine form of $K = K_0\,(1+\alpha\,\cos\,\omega t)$ to investigate why the earlier forms of $K\,(z,\,t)$ do not give the observed high supergeostrophic winds.

6. Analytical solutions of momentum equation

Writing

$$V = u + i\,v$$

$$W = V - G\,e^{ift} + G \tag{11}$$

Eq. (1) transforms to

$$\frac{\partial W}{\partial t} = K_0 . h(t)\,\frac{\partial^2 W}{\partial z^2} \tag{12}$$

To eliminate $h\,(t)$ define a modified time variable

$$T = \int_0^t h\,(t)\,dt \tag{13}$$

which reduces (12) to the standard form of parabolic equation.

$$\frac{\partial W}{\partial T} = K_0\,\frac{\partial^2 W}{\partial z^2} \tag{14}$$

The boundary conditions which were

$$(i)\ z = 0\ ,\ u = v = 0$$

$$(ii)\ z \to \infty,\ u \to G,\ v \to 0 \tag{15}$$

change to

$$(i)\ z = 0\ ,\ W(0,\,T) = G.[1 - \phi(T)]$$

$$(ii)\ z \to \infty,\ W \to G \tag{16}$$

(assumed invariant with time).

In Eq. (16), $\phi\,(T)$ as can be seen from Eq. (11) by putting $V=0$ is numerically equal to e^{ift} where T and t are uniquely related to each other through Eq.(13), for the type of functions one would normally encounter for $h(t)$. For the form $h(t) = 1 + \alpha\,\cos\,\omega t$ it is possible to find the inverse function $t = \psi\,(T)$ but it will not be the case in general.

An initial condition is now required. This may be imposed as Ekman spiral profile at $t=T=0$.

Explicitly, this is

$$W\,(z,0) = G.\left[\,1 - \exp\left\{\,-(1-i)\left(\frac{f}{2K}\right)^{\frac{1}{2}} z\,\right\}\,\right] \tag{17}$$

where K need not be equal to K_0

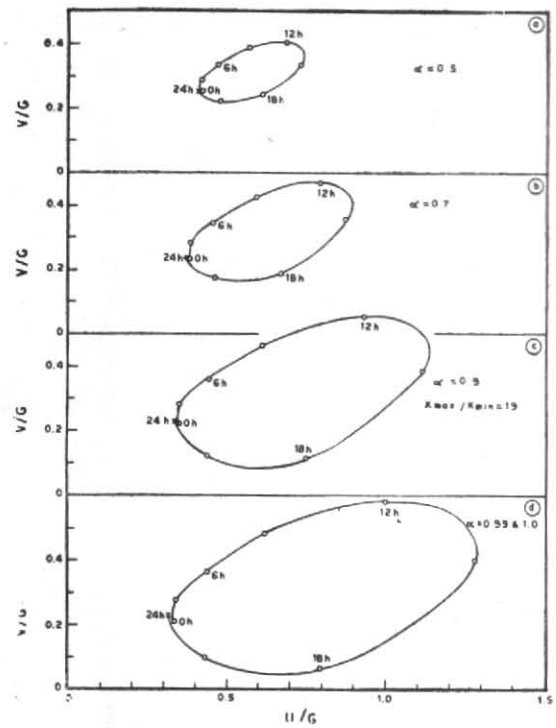

Fig. 5. Hodographs on second day of integration for $h\ (t) = 1+a \cos \omega t$ for various values of a. $K_0=10^5$ cm²/sec, $z=0{\cdot}3$ km, latitude=30°. The times refer to second day of integration, *e.g.*, 12 h represents $t=36$ hr

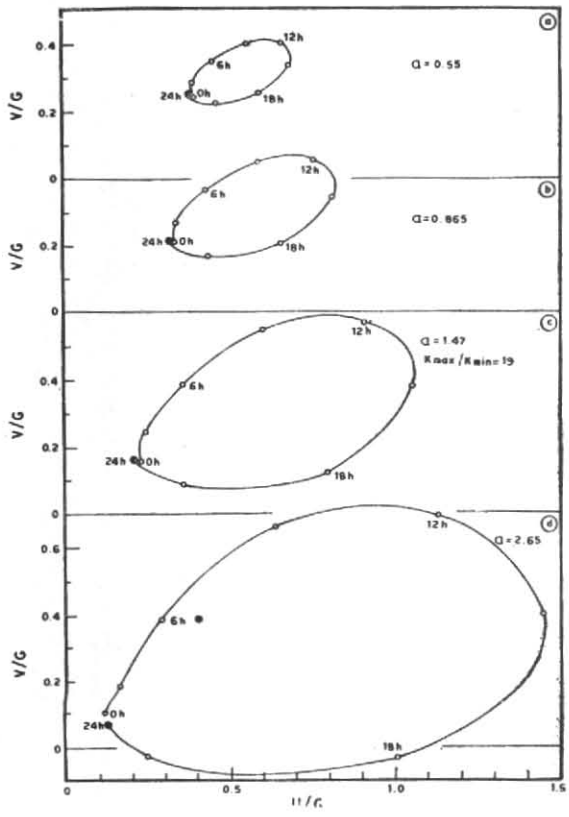

Fig. 6. Same as Fig. 5, but $h\ (t) = \exp\ (a \cos \omega t)$

From Carlsaw and Jaeger (1959) solution of Eq. (14) with boundary conditions given by Eq. (16) and initial condition given by Eq. (17) can be written as sum of two solutions

$$W = W_1 + W_2 \tag{18}$$

where W satisfies Eq. (14) with $W_1 = 0$ initially and $=W\ (0,T)$ at $z=0$ and W_2 satisfies Eq. (14) with $W_2 = W\ (z,0)$ initially and $W_2 = 0$ at $Z = 0$

We then have

$$W_1 = \frac{2G}{\sqrt{\pi}} \int_{z/2\sqrt{K_0 T}}^{\infty} \left[1 - \phi \left(T - \frac{z^2}{4K_0 \mu} \right) \right] e^{-\mu^2} d\mu \tag{19}$$

$$W_2 = \frac{G}{2\sqrt{\pi K_0 T}} \int_0^{\infty} F(z') \left[e^{-\frac{(z-z')^2}{4K_0 T}} - e^{-\frac{(z+z')^2}{4K_0 T}} \right] dz' \tag{20}$$

where,

$$F(z) = W\ (z,0)/G$$

Resubstituting

$$V = (W_1 + W_2 - G) e^{-ift} + G \tag{21}$$

u and v can then be obtained by separating real and imaginary parts of Eq. (21) for any given set of (z, t).

The main problem in evaluating the integrals is to obtain the value of t corresponding to a given value of T. In Eq. (19) the term $\phi\ (\tau)$ where

$$\tau = T - z^2/4K_0\mu^2$$

is simply e^{ift} where t corresponds to τ through Eq. (12). Thus, a graph of $T \rightarrow t$ using Eq. (17) is capable of giving ϕ if a graphical method is followed. Here, the evaluation was done using CDC 3600 computer.

7. Discussion of results

In Fig. 6, the solutions from Eq. (21) are presented in the form of hodographs at 0.3 km, 30° latitude and $K_0=10^5$ cm²/sec. These are for the linear cosine form of $K\ [h\ (t) = 1 + \alpha \cos \omega t]$ on the second day of integration. The points are at three hourly intervals. The value of α for each hodograph is also indicated. The hodographs are elliptical, conforming qualitatively to the observations. Initially, the amplitude of wind variations increases with the amplitude α of K – variations. However, an interesting feature is that as α approaches unity the wind oscillations reach an

upper limit as seen from the virtual congruence of the ellipses (Fig. 5d) for $\alpha = 0.99$ ($K_{max}/K_{min} = 199$) and $\alpha = 1$ (maximum possible amplitude).

The hodogarphs with $h(t) = e^{a \cos \omega t}$ for values of a corresponding to those in Fig. 5 such that K_{max}/K_{min} is same for both, are shown in Fig. 6, the other parameters being same. For small values of a, the corresponding ellipses are of the same size but the winds for the linear cosine case are a little higher.

7.1 *Supergeostrophic winds*

The hodograph in Fig. 6d with $a = 2.65$ corresponds to $\alpha = 0.99$. The remarkable feature of this hodograph is that the supergeostrophic wind at 0.3 km (not necessarily the jet level, is a little more than 1.5 G which is larger than, any values so far theoretically deduced. Thus the exponential cosine form (3) used here is capable of satisfying the Paegle's criterion cited earlier if suitable values of a are used to conform to the high summer amplitudes of K. In fact, for $a=3.3$ (about three times the mean spring amplitude) the supergeostrophic wind was 1.75 Gs. which is of the same order as the summer magnitudes of supergeostrophic winds at Great Plains.

7.2 *Profiles*

The profile of computed scalar wind approximately at the time of maximum jet (curves marked A) and at the time of maximum K (curves marked B) are shown in Fig. 7 for various forms of K (z, t) and latitudes. The time of maximum jet occurs after the time of occurrence of minimum K, the delay depending upon the inertial period *i.e.*, upon the latitude. As can be seen from Figs. 5 and 6, the delay is of about 2 hr at 30°. It is shorter, about one hour, for 60°. The A profiles which are profiles 3 hr after the occurrence of K_{min} at 30° and at the time of K_{min} at 60° are not significantly different from the maximum jet profiles. For the Cedar Hill profiles (*cf.* Fig. 4) the maximum jet occurs at 6 AM CST in spring. Its corresponding value in winter was 3 AM CST. In the case of analytical solutions, $t = 0$ refers to the time of occurrence of K_{max}. The mean value of this time as can be seen from Fig. 3 is about 1500-1600 hr CST. The time of the jet which at 30°, is 38 hr after K_{max} refers therefore to about 5 AM to 6 AM, which reasonably agrees with the observed time of occurrence of about 3 AM for predawn maxima, considering the simplified barotropic atmosphere assumed here.

The first two profiles (Fig. 7) are for the Cedar Hill spring and winter forms of K (z, t), and 30° latitude. The profiles marked 3 and 4 are for the exponential cosine form (9) with $K_0 = 10^5$ cm²/sec, for 30° and with $a = 1.1$ and 2.303 respectively. The former value of a is approximately same as the average $a(z)$ observed at Cedar Hill for spring and winter, and gives 18 fold diurnal change in K. The latter value of a is in conformity with the magnitude of a observed at Manor, Texas in summer and gives 100 fold diurnal change in K. The curves 5 and 6 are for the linear cosine form of K also with $K_0 = 10^5$ cm²/sec. The value of $\alpha = 0.8$ chosen for curve 5 gives the same 18 fold diurnal variation in K as for curve 3. Curve 6 is also for the linear cosine form with the same values of K_0 and α as for curve 5, but for Lat 60° N.

7.3 *Dimensional analysis*

Before proceeding to discuss these profiles, it would be desirable to examine the solution of Eq. (1) from considerations of dimensional analysis. If G is constant and form (9) is used for K, the solution of (1) can be formally written as

$$V/G = \phi\,(K_0, \omega, f, a, z, t) \tag{22}$$

If linear cosine form is used, then a gets replaced by α in (22).

In this expression, z and t are independent variables and the remaining four terms in the bracket are the four relevant parameters. From dimensional analysis, we can therefore write V/G as a function of four independent dimensionless combinations involving the five quantities. The parameter a however is already dimensionless and therefore the number of such combinations reduces to three. We can therefore write

$$V/G = \phi_1 \left\{ \left(\frac{f}{K_0}\right)^{\frac{1}{2}} z, ft, f/\omega, a \right\} \tag{23}$$

From the first quantity in the bracket in Eq. (23) we find that at any latitude, heights scale as $K_0^{\frac{1}{2}}$. In fact K_0 is the only quantity with which z is associated and this is the only scaling that can be observed without interference from other relevant parameters. Considering next the effect of a we note that this parameter is not coupled with any other variable and therefore the solutions for each value of a may be expected to be independent of the variations in other parameters, *i.e.*, they cannot be scaled. This is apparent from curves 3 and 4. It is also interesting to note that the jet level is lower for higher value of a.

The maximum jet speeds are 1.6 G and 1.34 G for profiles 4 and 3 respectively.

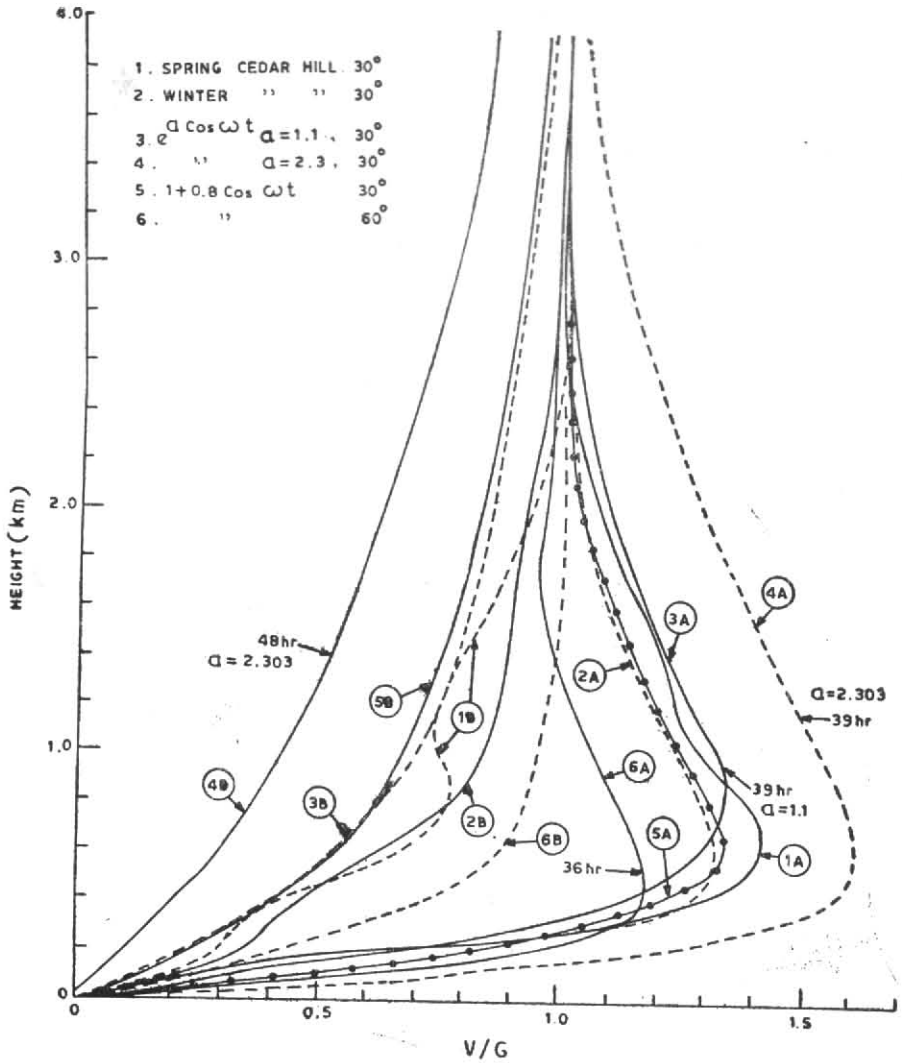

Fig. 7. Comparison of the wind profies approximately at the time of maximum jet (A) and at the time of maximum K (B) using various forms of $K(z,t)$. Except for the first two profiles, the solutions are analytic and hence do not converge at 4 km, the artificial infinity for the numerical solutions.

Comparing next the profile 5A with 3A, we note that here also, the jet level for the linear cosine form is lower than that for exponential cosine, though the magnitude of the jet is approximately same. Because of the complicated nature of the oscillations involving a number of independent parameters the height of the jet level does not scale exactly in the ratios of square roots of $K_{\min}$.

7.4 *Latitude dependence*

The dependence of solutions on latitude comes through the coriolis term f. From the first term in the brackets in Eq. (23) it is seen that height scaling may be made through the term $\int^{-\frac{1}{2}}$. However, a straightforward scaling cannot be expected because of the interference from ω and time terms. The dependence of the amplitude of the wind oscillations on the term f/ω was confirmed by obtaining the solutions at 15° and comparing them with solutions obtained by putting 2ω instead of ω in the linear cosine form of $K(z,t)$. The hodographs in both the cases were almost identical The quantity $|\ 1 - f/\omega\ |$ becomes approximately same in both the cases. This quantity also enters the solution given by Buajitti and Blackadar (1957). A weak resonance indicated by this term, in the amplitude of oscillations was also observed at 30° where $f=\omega$. All other parameters remaining same, the amplitudes of wind oscillations decreased slowly on either side of 30°. This may be contrasted with the comparatively sharp fall in the amplitude of wind oscillations observed by Paegle (*loc. cit*) in his calculation of thermal wind oscillations at 37° instead of 30° by Holton's model (Holton 1964). Supergeostrophic winds decrease with latitude above 30°. Thus, as compared with 1.6 G at 30° for $a = 2.303$, the value was only 1.5 G

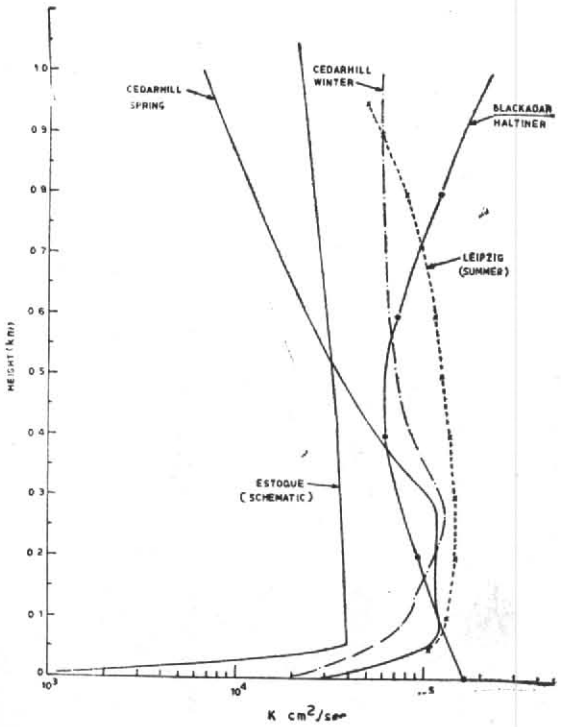

Fig. 8. Comparison of various forms of mean daily profiles of the eddy transfer coefficient in the planetary boundary layer

at 45°. Similarly using the linear cosine form of K with $\alpha = 0.8$, the maximum jet wind is $1.34\ G$ at 30° but only $1.27\ G$ at 60° as seen from the profiles 5 B and 6 B in Fig. 7. These curves also show a significant feature that the height of the maximum jet wind decreases with latitude and the height of the planetary boundary layer (*i.e.*, the layer in which K affects the wind field) also decreases similarly.

7.5 *Height dependence of K*

We shall now compare the profiles 1 and 2 obtained with z-dependent K with profiles 3 and 5 for z-independent K. It may be recalled that the value of a in profile 3 is same as the mean $a(z)$ for Cedar Hill profiles and K_{max}/K_{min} for profiles 3 and 5 are identical.

The irregular nature of 1B and 2B may be ascribed to the corresponding irregularity in the K–profile. Comparatively, the profiles at the time of maximum jet show this feature to a lesser extent in spring and do not show at all in winter.

The effect of z-dependence of K is seen to be felt more in the upper layers. When K decreases with height, (profiles 1 and 2) the profiles converge fast at about 2.5 km level. However, for height independent K amplitude of oscillation is significant at these levels and increases with amplitude of K, apparently giving unrealistically high values of planetary boundary layer. It appears therefore that K should decrease fast at upper levels.

8. Concluding remarks

It is thus seen that the exponential cosine form of $K\ (z, t)$ with proper parameters for amplitude of K is capable of generating the observed magnitudes of supergeostrophic winds. The Cedar Hill $K(z, t)$ deduced from the Fourier analysis of $\log K$ is therefore a step towards obtaining the correct picture of the diurnal variations of $K(z, t)$ and wind in the planetary boundary layer though it must be noted that the actual phenomena may be much more complex than that depicted by the simple model used here. In Fig. 8 we compare the mean daily profiles obtained from the Cedar Hill $K\ (z, t)$ with those of others. The qualitative agreement with the Leipzig profile and Estoque's profile lend some support to the functions used in this work, though the functions are purely empirical. Haltiner's K profile obtained from Blackadar's 6 hourly observations is the only exception to the general behaviour of the K-profile and is rather enigmatic. It is felt from the present work that six hourly observations are not adequate to deduce $K\ (z, t)$. This may be seen

from Figs. 5 and 6 where the maximum winds do not occur at the time of K_{min}, but after it, the delay depending upon the latitude, that at 30° being about 3 hours. This is due to the inertial lag determined by the coriolis parameters. The problem is however open and scope exists for repetition of Blackadar's pioneering experiments but with the observation intervals reduced to one hour or less and extended to cover all the seasons of the year.

REFERENCES

Blackadar, A. K.	1957	*Bull. Amer. met. Soc.*, **38**, pp. 283-290.
	1959	Final Rep. Study of forecasting low level wind gradients, AFCRE-R-59-220, Pennsylvania State Univ.
Buajitti, K. and Blackadar, A. K.	1957	*Quart. J. R. met. Soc.*, **83**, pp. 486-500.
Carlsaw, H. S. and Jaeger, J. C.	1959	*Conduction of Heat in Solids.* Ch. II, Oxford Univ. Press, 2nd Ed. 510 pp.
Estoque, M. A.	1963	*J. geophys. Res.*, **68**, pp. 1103-1113.
Gill, S.	1952	*Camb. Phil. Soc. Meet.*, **47**, pp. 96-108.
Haltiner, C. J.	1959	*Tellus*, **11**, pp. 452-458.
	1960	*Ibid.*, **12**, pp. 357.
	1961	*Ibid.*, **13**, pp. 438-439.
Holton, J. R.	1967	*Ibid.*, **19**, pp. 199-205.
Jehn, K. H. and Gerhardt. J. R.	1950	*J. Met.*, **7**, pp. 343-346.
Lettau, H.	1950	*Tellus*, **2**, pp. 125-129.
McBride, J. R.	1960	Determination of the coefficient of eddy viscosity as a function of height and time, and separately as a function of stability and vertical shear of the wind. *U.S. Naval Postgraduate School Thesis.*
Paegle, J.	1970	Studies of diurnally periodic boundary layer winds. *Tech. Rep. to NSF*, Univ. California.
Wagner, A.	1939	*Beirtrage Physik fr. Atm.*, **25**, pp. 145-170.
Wong, E. Y. J. and Brundidge, K. C.	1966	*J. Met.*, **23**, pp. 167-178.